processes

MDPI

Article

A Fault Direction Criterion Based on Post-Fault Positive-Sequence Information for Inverter Interfaced Distributed Generators Multi-Point Grid-Connected System

Fan Yang [1], Hechong Chen [1], Gang Han [1], Huiran Xu [2], Yang Lei [1], Wei Hu [1] and Shuxian Fan [2,*]

[1] State Grid Hubei Electric Power Co., Ltd., Wuhan 430077, China; yangf_82@163.com.cn (F.Y.); chenhc16@hb.sgcc.com.cn (H.C.); hghangang12@163.com (G.H.)
[2] College of Electrical Engineering and Automation, Shandong University of Science and Technology, Qingdao 266590, China; xuhuiran@163.com
* Correspondence: fanshuxian@163.com

Abstract: In response to the poor reliability in identifying fault direction in distribution networks with Inverter Interfaced Distributed Generators (IIDGs), considering the control strategy of low-voltage ride-through, a fault direction criterion based on post-fault positive-sequence steady-state components is proposed. Firstly, the output steady-state characteristics of IIDGs considering the low-voltage ride-through capability are analyzed during grid failure, and the applicability of existing directional elements in a distribution network with IIDGs connected dispersively is demonstrated. Subsequently, for the typical structure of an active distribution grid operating under flexible modes, the positive-sequence voltage and current are examined in various fault scenarios, and a reliable direction criterion is suggested based on the difference in post-fault positive-sequence impedance angles on different sides of the lines that are suitable whether on the grid side or the IIDG side. Lastly, the reliability of the proposed direction criterion is verified by simulation and the results indicate that the fault direction can be correctly determined, whereas phase-to-phase and three-phase short circuit faults occur in different scenarios, independent of the penetration and grid-connected positions of IIDGs, fault location, and transition resistance. It is suitable for fault direction discrimination of an IIDGs multi-point grid-connected system under a flexible operation mode.

Keywords: renewable energy system; IIDG; positive-sequence component; direction criterion; flexible operation mode

Citation: Yang, F.; Chen, H.; Han, G.; Xu, H.; Lei, Y.; Hu, W.; Fan, S. A Fault Direction Criterion Based on Post-Fault Positive-Sequence Information for Inverter Interfaced Distributed Generators Multi-Point Grid-Connected System. *Processes* **2024**, *12*, 1522. https://doi.org/10.3390/pr12071522

Academic Editor: Maoyin Chen

Received: 19 June 2024
Revised: 12 July 2024
Accepted: 16 July 2024
Published: 19 July 2024

1. Introduction

To ensure the selectivity and reliability of active distribution network protection with IIDGs connected dispersively, the widely adopted scheme is to increase directional elements on the existing current protection [1–3] or to apply distance protection or longitudinal protection based on fault direction discrimination information [4–6], among which accurate direction discrimination is the key to influence the correct action of protection. Traditional directional elements are suitable for power grids with a single power type and stable operation. However, in an active distribution network with dynamic changes in network structure, operation mode, and fault characteristics, the performance of the traditional directional elements may be degraded, and they may fail because of the strong coupling nonlinear connection between the IIDG output current and the PCC voltage [7–10]. Therefore, it is necessary to study a new fault direction criterion.

At present, many research results on a direction criterion for different application scenarios in active distribution networks have been achieved. The fault direction is determined by extracting the current phases of any two feeders on the bus in [11] and the current phases of the fault components with more than three lines on the bus are used, and

the sensitivity is high [12]. In [13], the fault range is reduced to a fault search area by comparing the current amplitudes at multiple locations, and then the fault direction is judged using the phase relationship of the currents in the area, which has good adaptability to the change in the network structure. The methods are based on multi-position information and cannot meet the requirements of local protection. In [14], the phase difference between the positive-sequence currents before and after fault is adopted without considering the IIDG control mode, and it is not suitable for cases where there are branches in the line. Furthermore, taking the quantity defined by the positive-sequence fault component of the measured current as a reference value, the fault component phase is compared to determine fault direction [15], which is not only applicable to any line whether there are branches or not, but also is not affected by the load current. However, because IIDG is equivalent to the series of voltage sources and impedance, it is not suitable for on-site operation to make the application limited. In [16], based on the fact that the upstream current provided by the system is greater than the downstream current provided by IIDGs, direction discrimination is achieved on the grid side and IIDG side according to different direction discrimination logics using a short circuit current only, but the protection may fail when the system operation mode changes. In [17], considering that the fault current lags behind the voltage when a fault occurs in the positive direction, the fault direction is judged, but misjudgment is inevitable if the premise is not met. The direction reference symbol is constructed based on the zero-crossing characteristics of the prefault current to determine fault direction in [18], but it is not suitable for the scenario where the reverse power flow may occur. The methods are effective only for certain application scenarios and the flexibility is poor. A direction criterion using the phase information of a positive-sequence fault current and prefault voltage is proposed considering a photovoltaic power supply with low-voltage ride-through capability connected to the distribution network in [19], and the positive-sequence fault current and voltage are extracted to form a criterion in [20]. However, the action areas of directional elements are asymmetric, and the criteria on both sides are different, which cannot be applied to the flexible operation mode.

This article focuses on the typical structure of an IIDG multi-point grid-connected system with low-voltage ride-through capability, analyzes the positive-sequence fault characteristics of each protection on the grid side under different scenarios, extracts coherent features in the same fault direction upstream and downstream of the fault point, and forms a universal direction criterion based on the positive-sequence impedance angle. At last, simulation analysis shows that the proposed criterion is reliable. The work can provide technical support for improving the protection of active distribution networks.

2. Analysis of Output Characteristics of IIDG with Low-Voltage Ride-Through Capability

The output characteristics of IIDG depend on the control method and current limiting technique. IIDG is also required to have low-voltage ride-through capability; that is, when the grid-side voltage decreases to varying degrees, IIDG will not disconnect from the grid within a certain time and will prioritize outputting a certain amount of reactive power to support the grid voltage [20]. Therefore, IIDG will often adopt a PQ decomposition control strategy to control active and reactive power output flexibly and perform negative-sequence suppression to only output positive-sequence components, and current-limiting measures make its maximum output current no greater than 1.2 times the rated current. According to the above analysis, IIDG can be equivalent to a current source controlled by the positive-sequence voltage of the point of common coupling (PCC), shown in Figure 1.

In Figure 1, the IIDG output positive-sequence currents is $\dot{I}_{\mathrm{DG}}$, $\dot{U}^{+}_{PCC}$ is the positive-sequence voltage at PCC and its phase angle is γ, and the relationship can be expressed as $\dot{I}_{\mathrm{DG}} = \left(I_{dref}\cos\gamma + I_{qref}\sin\gamma\right) + j\left(I_{dref}\sin\gamma - I_{qref}\cos\gamma\right)$, where I_{dref} and I_{qref} are the reference values for the output active and reactive current of IIDG. The phase angle of the positive-sequence voltage ahead of the IIDG output current is φ_{DG}, $\varphi_{\mathrm{DG}} = \arctan\left(I_{qref}/I_{dref}\right)$ [20].

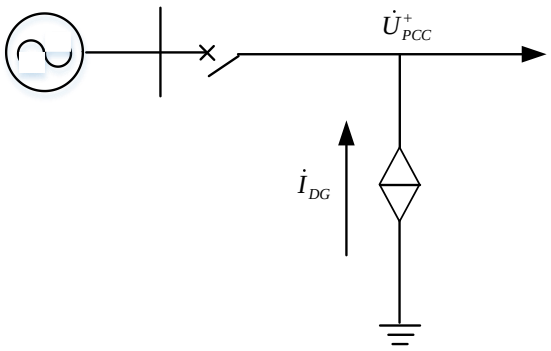

Figure 1. The IIDG equivalent model.

The active and reactive current output of IIDG satisfy Equations (1) and (2), respectively [21]:

$$\begin{cases} I_{qref} = 0 & \frac{U^{+}_{PCC}}{U_N} > 0.9 \\ I_{qref} \geq 1.5 I_N (0.9 - \frac{U^{+}_{PCC}}{U_N}) & 0.2 < \frac{U^{+}_{PCC}}{U_N} \leq 0.9 \\ I_{qref} = 1.05 I_N & \frac{U^{+}_{PCC}}{U_N} \leq 0.2 \end{cases} \tag{1}$$

$$\begin{cases} I_{dref} = \frac{S_N}{U^{+}_{PCC}} & \frac{U^{+}_{PCC}}{U_N} > 0.9 \\ I_{dref} = \sqrt{I^2_{\max} - I^2_{qref}} & \frac{U^{+}_{PCC}}{U_N} \leq 0.9 \end{cases} \tag{2}$$

In Equation (1), I_N is the rated current of IIDG, and U_N is the grid-rated phase voltage. In Equation (2), S_N is the IIDG single-phase rated output power under normal operation, and $I_{\max}$ is the maximum output current value of IIDG. Usually, the amplitude of the IIDG output current is limited to $1.2I_N$. According to Equation (1), with a smaller U^{+}_{PCC}, larger I_{qref}, and maximum value of $1.05I_N$, then I_{dref} is equal to $0.58I_N$. In this case, the maximum φ_{DG} is 61.1°, and the minimum value is 0°.

3. Analysis of the Applicability of Conventional Directional Elements

Traditional directional elements mainly adopt a direction criterion based on 90° wiring and the positive-sequence fault component criterion. The theoretical basis for the 90° wiring directional element is that the phase angle of the line-to-line voltage, including the non-faulted phase voltage, leads the faulted phase current to be within limits when fault occurs in the positive direction of the element, and the operation criterion can be expressed as follows [22]:

$$-90^\circ \leq \varphi_k + \alpha \leq 90^\circ \tag{3}$$

where φ_k is the angle at which the measured line-to-line voltage leads to the phase current, and α is the internal angle of the directional element.

During grid failure, the output of IIDG may affect the voltage and current on the grid side, and the measured voltages and currents of the 90° wiring directional element may change, leading to a misjudgment of fault direction.

The conventional direction criterion based on positive-sequence fault components is that the phase angle at which the positive-sequence voltage fault component leads the current is within limits when fault occurs in the positive direction, and the operation criterion can be expressed as follows [23]:

$$-90^\circ \leq \arg(\frac{\Delta \dot{U}_1}{-\Delta \dot{I}_1}) - \varphi_{sen} \leq 90^\circ \tag{4}$$

where $\Delta \dot{U}_1$ and $\Delta \dot{I}_1$ represent the positive-sequence fault components of voltage and current, respectively, and φ_{sen} is the maximum sensitivity angle.

For the above directional element, the uncertainties of the line current under normal operation and the post-fault current considering the effects of IIDGs may both cause the misjudgment of fault direction.

A 10 kV distribution network with IIDGs interconnected to PCC dispersively is constructed in Figure 2. The system parameters are as follows: line impedance angle is 70°, the length of each section is 2 km, the load capacity is 1.2 MVA, and the capacity of each IIDG is 727 kVA. Assuming that a three-phase short circuit with transition resistance 10 Ω or a phase-to-phase short circuit occurs at the midpoint f of line CD, the actions of conventional elements are simulated and analyzed.

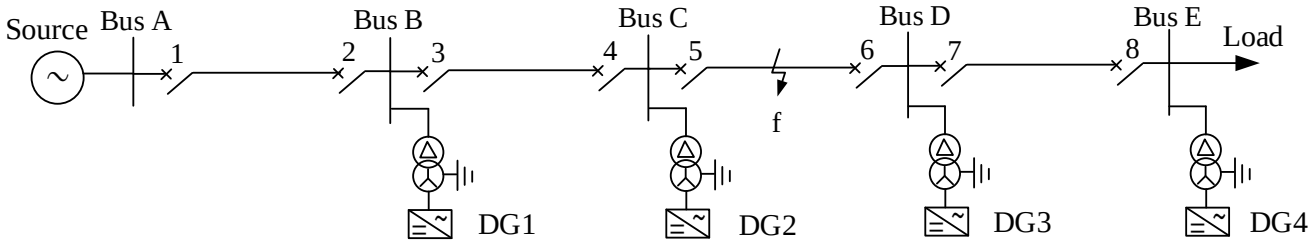

Figure 2. The structure diagram of the distribution network with IIDGs connected dispersively.

Table 1 shows the measured values of directional elements for 90° wiring, from which it can be seen that there will be a misjudgment of the fault direction at Protection 7 and 8 downstream of the fault point. Table 2 shows the measured values of positive-sequence fault component directional elements, from which it can be seen that there are misjudgments in all the directional elements upstream and downstream of the fault point. In addition to the impacts of IIDGs after the failure on the grid side, it is also related to the reverse flow of power before the failure. Therefore, it is necessary to propose a direction criterion in a distribution network with IIDGs connected dispersively.

Table 1. Measured values of the 90° wiring directional elements.

Short Circuit Fault Type	Measured Value	1	2	3	4	5	6	7	8
Three-phase	$\arg\frac{U_{AB}}{I_C}$	−35°	144°	−36°	143°	−37°	−78°	**19°**	**203°**
	$\arg\frac{U_{BC}}{I_A}$	−35°	−216°	−36°	−217°	−37°	−78°	**19°**	**−156°**
	$\arg\frac{U_{CA}}{I_B}$	325°	144°	324°	143°	323°	282°	**19°**	**203°**
Phase-to-phase (BC)	$\arg\frac{U_{AB}}{I_C}$	14°	189°	14°	184°	35°	−44°	**−19.5°**	**151°**
	$\arg\frac{U_{CA}}{I_B}$	317°	142°	322°	147°	327°	267°	**48°**	**229°**

Bold fonts indicate errors in the judgment of traditional directional elements.

Table 2. Measured values of directional elements based on positive-sequence fault components.

Short Circuit Fault Type	Measured Value	1	2	3	4	5	6	7	8
Three-phase	$\arg\frac{\Delta\dot{U}_1}{-\Delta\dot{I}_1}$	**−113°**	**54°**	**−126°**	**51°**	**−130°**	**−138°**	**54°**	**−126°**
Phase-to-phase (BC)	$\arg\frac{\Delta\dot{U}_1}{-\Delta\dot{I}_1}$	**−115°**	**53°**	**−127°**	**51°**	**−129°**	**−141°**	**62°**	**−118°**

Bold fonts indicate errors in the judgment of traditional directional elements.

4. A Fault Direction Criterion Based on Post-Fault Positive-Sequence Components

4.1. Change in Positive-Sequence Impedance Angle after Grid Failure

The positive-sequence components will exist in the power grid no matter what type of fault occurs, and fault direction identification using only the post-fault positive-sequence components is unrelated to the uncertain prefault power flow. Therefore, it is advised to analyze the positive-sequence impedance angle measured by each directional element on

the grid side in order to find the difference when a fault occurs in the positive or negative direction relative to each element depicted in Figure 2.

The system power supply is usually equivalent to a constant voltage source $\dot{E}_S$ in series with equivalent impedance, and it outputs positive-sequence components only. Its positive-sequence and negative-sequence equivalent impedance are basically equal, expressed as Z_S. Because the lines are static elements, the positive-sequence impedance is equal to the negative-sequence impedance, which can be uniformly expressed by the same symbols. Z_{AB}, Z_{BC}, and Z_{DE} represent the equivalent impedance of lines AB, BC, and DE, respectively, and the line impedance from bus C to the fault point is equivalent to Z_{Cf}, and it is Z_{fD} from bus D to the fault point. The positive-sequence and negative-sequence impedance of load are basically equal, expressed as Z_L, and usually much larger than the line impedance. According to part 1, IIDGs are considered to be voltage-controlled current sources and output positive-sequence components only, so the output positive-sequence currents of IIDG1–4 are $\dot{I}_{DG1}$, $\dot{I}_{DG2}$, $\dot{I}_{DG3}$, and $\dot{I}_{DG4}$, varying with the voltages of each grid-connected point. The post-fault positive-sequence network (Figure 3) and negative-sequence network (Figure 4) are established when phase-to-phase short circuit fault occurs at f.

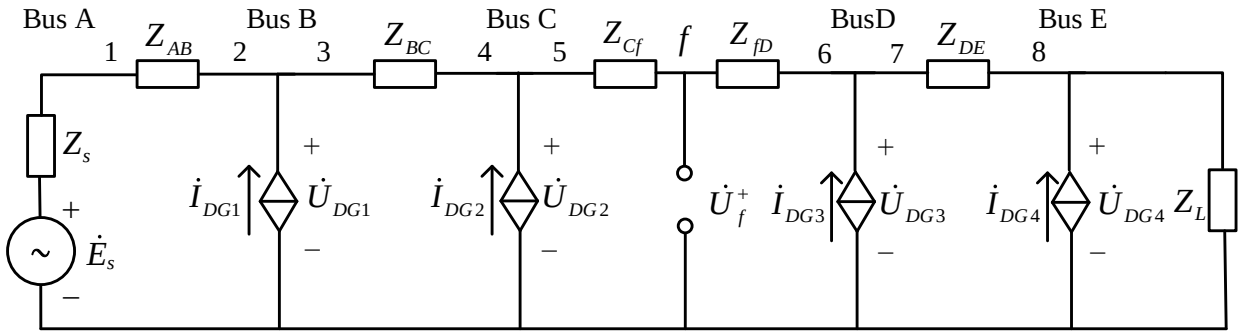

Figure 3. Positive-sequence equivalent network.

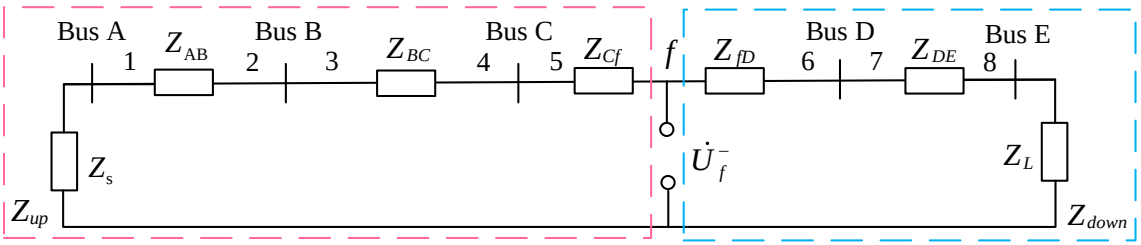

Figure 4. Negative-sequence equivalent network.

Where $\dot{U}_{DG1}$~$\dot{U}_{DG4}$ represent the voltages at PCC of IIDG1–4, Z_{up} denotes the upstream equivalent impedance with $Z_s + Z_{AB} + Z_{BC} + Z_{Cf}$, Z_{down} is the downstream impedance with $Z_{fD} + Z_{DE} + Z_L$, and Z_{down} is far greater than Z_{up}. Taking the fault point as the port, the equivalent negative-sequence impedance is equal to the parallel impedance of Z_{up} and Z_{down}, expressed as Z_f^-, and it is almost equal to Z_{up}. $\dot{U}_f^+$ and $\dot{U}_f^-$ are the positive-sequence and negative-sequence voltages at f. It is well-known that $\dot{U}_f^+$ is equal to $\dot{U}_f^-$ when phase-to-phase short circuit fault occurs, and then a compound sequence network (Figure 5) is formed.

For long-distance faults on heavy load lines, Z_L will decrease when the upstream line impedance of the fault point increases. Z_f^- will be significantly less than Z_{up}.

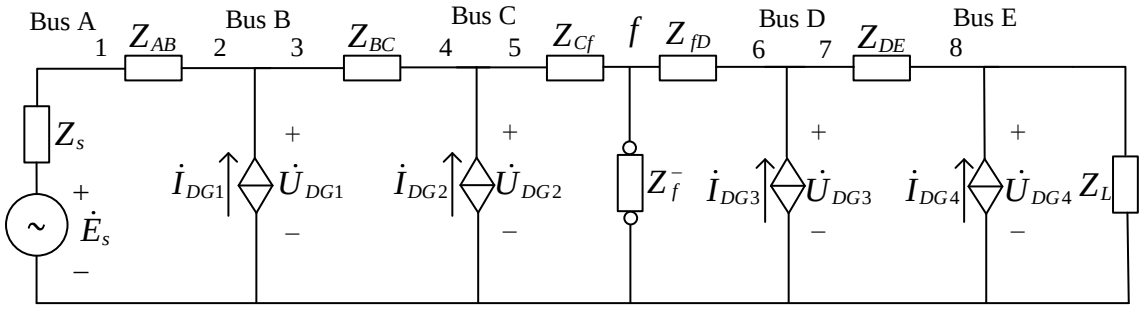

Figure 5. Compound sequence network.

For the upstream network, the short circuit current is mainly provided by the system power supply because of the large capacity, flowing to the fault point, and the voltage phase is almost constant. Therefore, for elements 1, 3, and 5, the positive-sequence voltage phase is the line impedance angle ahead of the current phase, ignoring the influence of IIDGs. Generally, the line impedance angle is 0°~90°, so the measured positive-sequence impedance angle fulfills Equations (5) and (6).

Positive direction fault (for elements 1, 3, and 5):

$$0^\circ < \arg\frac{\dot{U}_{\mathrm{m1}}}{\dot{I}_{\mathrm{m1}}} \le 90^\circ \tag{5}$$

Reverse direction fault (for elements 2 and 4):

$$180^\circ < \arg\frac{\dot{U}_{\mathrm{m1}}}{\dot{I}_{\mathrm{m1}}} \le 270^\circ \tag{6}$$

In Equations (5) and (6), $\dot{U}_{m1}$ and $\dot{I}_{m1}$ represent the measured positive-sequence voltage and current.

If a phase-to-phase short circuit occurs, Z_{f}^- is approximately equal to the upstream positive-sequence impedance and much less than the downstream load impedance in Figure 5. According to the superposition theorem, the system voltages and currents are superimposed by the electrical quantities generated by each power supply. If only the upstream power supply is powered, the short circuit current mainly flows through Z_{f}^- to form the main short circuit loop, and the downstream current is relatively small. Therefore, according to the principle of voltage distribution in a short circuit loop, the voltage at f is slightly less than 0.5 times the rated voltage, and the downstream voltage decreases gradually. When IIDG is powered separately, the currents flowing to both sides of PCC are inversely proportional to the equivalent impedance on both sides, and the current flowing towards the system side is relatively large due to the smaller impedance. The larger the IIDG capacity, the greater the current provided. When the load is heavy, the short circuit current flowing to the load side provided by the system power supply will increase. Meanwhile, if the IIDG capacity is small, such as IIDG3, the current flowing to the system side provided by it may be smaller than the current flowing downstream provided by the upstream power supply of the fault point. Under the combined action of the system power supply and IIDG3, the superimposed current will flow downstream of element 6, and the fault direction of element 6 must be misjudged. However, since the current amplitude is small in this case, current protection will not malfunction, and the directional element can also be directly locked according to the smaller current amplitude. If the IIDG capacity is large enough, the superimposed current flowing through element 6 is from the bus to the fault point, and the current amplitude is also larger than the starting value at the same time, so the directional element can start normally, and direction discrimination is carried out after that.

Therefore, the premise for direction discrimination is that the downstream current flows towards the fault point when a phase-to-phase short circuit occurs, and the following analysis is carried out in this condition. Since the downstream voltage is approximately equal to 0.5 times the rated voltage now, the output currents of the downstream IIDGs are calculated to lag behind the grid voltage by about 13° according to Equations (1) and (2). The current flowing through line ED is $\dot{I}_{DG4}$, and its maximum output current value is less than 1.5 times the load current value of the connected line if the permeability of IIDG is 100%. Therefore, the voltage drop in line ED does not exceed 10.5% of U_{DG4}. Taking $\dot{U}_{DG4}$ as the reference phasor, according to the equation $\dot{U}_{DG3} = \dot{U}_{DG4} - \dot{I}_{DG4}Z_{ED}$, the phasor diagram for each node voltage and branch current is plotted as shown in Figure 6. Given that the impedance angle of Z_{ED} ranges from 0° to 90°, the phase range of $\dot{I}_{DG4}Z_{ED}$ is bounded by the pink-colored phasor shown in the figure. Combined with its amplitude characteristics, the cosine theorem is used to calculate that $\dot{U}_{DG3}$ lags behind $\dot{U}_{DG4}$ by about −2°~6°, with a voltage drop of no more than 10.2%. Due to uncertainties in the system operation mode and line parameters, each phasor fluctuates within a certain range, and the shadow region of each color represents the boundary of the definition domain for each phasor.

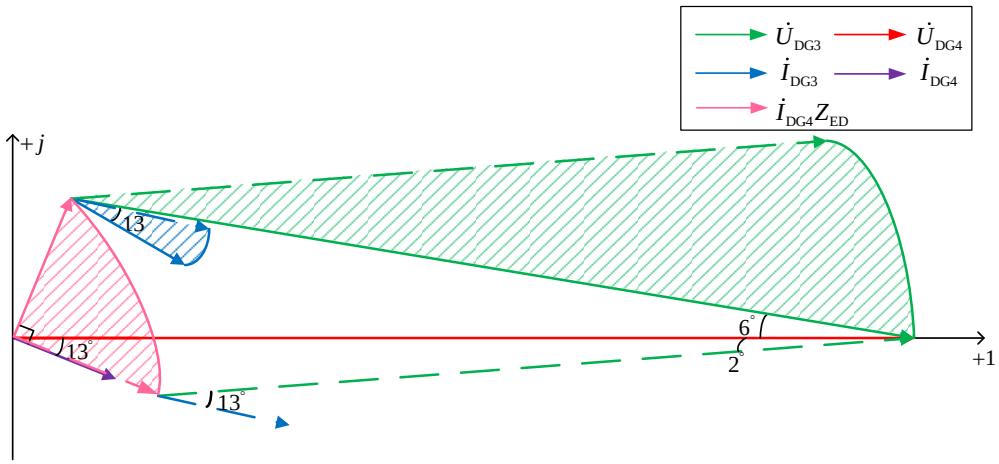

Figure 6. The phasor diagram of the downstream voltages and currents when a phase-to-phase fault occurs.

In the analysis process, the penetration of IIDG at PCC is considered as 100%, and the voltage drop along the line takes the maximum possible value, with a large margin. Thus, if there are more IIDGs downstream, the same conclusion can be obtained. For the downstream elements 6, 7, and 8, the measured positive-sequence voltage is $\dot{U}_{DG3}$, $\dot{U}_{DG3}$, and $\dot{U}_{DG4}$, respectively, and the measured current is $(\dot{I}_{DG3} + \dot{I}_{DG4})$, $-\dot{I}_{DG4}$, and $\dot{I}_{DG4}$. Hence, the phase difference of positive-sequence voltage and current satisfies Equations (7) and (8):

Positive direction fault (for elements 6 and 8):

$$-8^\circ \leq \arg\frac{\dot{U}_{m1}}{\dot{I}_{m1}} < 21^\circ \tag{7}$$

Reverse direction fault (for element 7):

$$174^\circ \leq \arg\frac{\dot{U}_{m1}}{\dot{I}_{m1}} < 195^\circ \tag{8}$$

If a three-phase short circuit occurs, Z_f^- in Figure 5 becomes zero, and the voltage at f is zero, while the downstream current flows from the IIDGs to the fault point. The IIDGs' output power is almost entirely consumed in the line from PCC to the fault point. Even

with a 100% penetration rate of IIDGs, the voltage drop of its maximum output current along the line is less than 10.5% of the rated voltage. It implies that the voltage at each PCC will be lower than 0.2 times the rated voltage, and thus the IIDG output current will reach its maximum value, with the output current phase lagging behind the voltage at PCC by 61.1°.

At this time, all the reactive power output by the downstream IIDGs and the line-to-ground capacitance from PCC to the fault point is consumed by the line equivalent inductance. Therefore, the output current frequency of IIDGs can be derived as follows [24]:

$$f = \frac{-Q_{DG} + \sqrt{Q_{DG}^2 + 4P_{DG}^2 R^2 C/L}}{4\pi C P_{DG}\sqrt{R}} \tag{9}$$

where P_{DG} and Q_{DG} are the output active and reactive power of the downstream IIDGs, and R, L, and C represent the line equivalent resistance, inductance, and line-to-ground capacitance from PCC to the fault point, respectively. Because the line impedance is inductive, R is very small, and C can be ignored, it will result in a significant rise in system frequency and the angle of line equivalent impedance will be close to 90°.

Figure 7 shows a phasor diagram of the downstream currents and voltages. Assuming $\dot{U}_{DG4}$ as the reference phasor and considering $\dot{U}_{DG3} = \dot{U}_{DG4} - \dot{I}_{DG4}Z_{ED}$, the voltage drop along line ED will not exceed U_{DG4}, and it can be concluded that $\dot{U}_{DG3}$ falls within the range of −75.6°~0°, and the angle that $\dot{I}_{DG3}$ lags behind $\dot{U}_{DG3}$ is 61.1°. Therefore, the domain of positive-sequence impedance angle detected by element 7 is 166°~242°, while that detected by element 6 is −14.5°~61.1°.

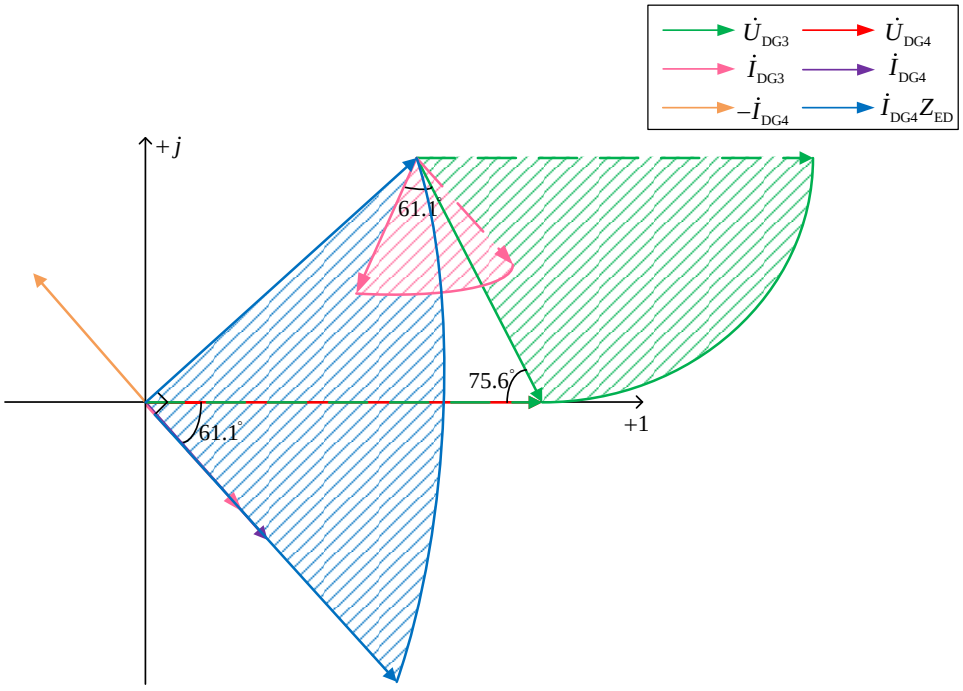

Figure 7. The phasor diagram of the downstream voltages and currents when a three-phase short circuit occurs.

The angle of the positive-sequence impedance measured by each downstream directional element satisfies Equations (10) and (11).

Positive direction fault (for elements 6 and 8):

$$-15^\circ \le \arg\frac{\dot{U}_{m1}}{\dot{I}_{m1}} \le 62^\circ \tag{10}$$

Reverse direction fault (for element 7):

$$166^\circ < \arg\frac{\dot{U}_{m1}}{\dot{I}_{m1}} \leq 242^\circ \tag{11}$$

As the system structure changes, i.e., a closed-loop structure with an open-loop operation or the lines in the distribution network are only equipped with switches and directional elements on the grid side, the analysis results of positive-sequence impedance angle are still as mentioned above according to the analysis method used. It will not be repeated in this paper.

4.2. Fault Direction Criterion Based on the Positive-Sequence Impedance Phase

The research indicates that the voltage–current relationship along the lines becomes more complex due to the strong coupling relationship between the voltage at PCC and the output current of IIDG. Based on the analysis results under various scenarios and fault types, a universal criterion for directional elements can be formed:

Positive direction fault:

$$-45^\circ < \arg\frac{\dot{U}_{m1}}{\dot{I}_{m1}} \leq 135^\circ \tag{12}$$

Reverse direction fault:

$$135^\circ < \arg\frac{\dot{U}_{m1}}{\dot{I}_{m1}} \leq 315^\circ \tag{13}$$

The proposed direction criterion fully considers the influence of the distribution line parameter, fault type, grid-connected location and capacity of IIDG, and low-voltage ride-through capability, and it has a large margin and high sensitivity.

The process of direction discrimination is shown schematically in Figure 8.

(1) When any phase current measured by a directional element is greater than twice the maximum load current, the directional element starts.
(2) Collect the data of three-phase steady-state voltage and current within the time window tw after t starting from system failure, and calculate the positive-sequence voltage and current, where t = 20 ms and tw = 20 ms. Among them, the current data must be the three-phase current flowing from the directional element to the protected line.
(3) If the recorded positive-sequence voltage meets $U_{m1} \leq 2\%U_N$, the voltage data from 20 ms before the fault are utilized for calculation, avoiding voltage dead zone issues in case of a three-phase short circuit at the line outlet.
(4) Calculate the phase difference of the positive-sequence voltage and current, denoted as $\Delta\varphi$.
(5) Compare $\Delta\varphi$ with the threshold of direction criterion, and if Equation (12) is satisfied, it is judged as a positive direction fault; if Equation (13) is satisfied, it is determined to be a reverse direction fault.

The criterion based on local information needs to collect the local voltage and current data before and after the fault at the protection installation, then calculate the positive-sequence voltage and current phasor with less calculation. In order to avoid the influence of the transient process, the data of one cycle after 20 ms of the fault are collected, so the data acquisition and processing time will not be more than 50 ms, and not affect the quickness of the distribution network protection.

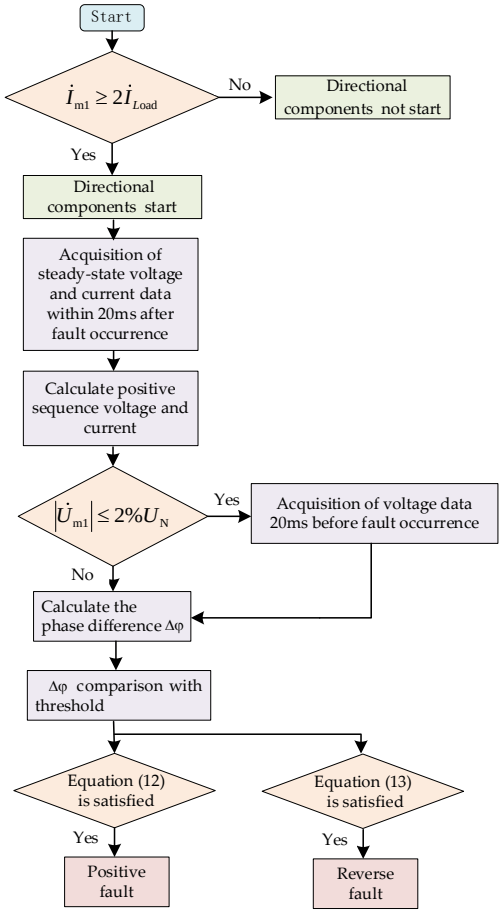

Figure 8. The flow chart of direction criterion based on the positive-sequence components.

5. Case Analysis

A simulation model of a 10 kV distribution network is established as shown in Figure 1 [25,26]. The line positive-sequence impedance is (0.13 + j0.35) Ω/km. The length of line AB is 2 km, and IIDG1 is connected to bus B with a rated output power of 303 kVA; line BC is 4 km, and IIDG2 is connected to bus B with the same capacity. The length of line CD and DE is 2 km and 5 km, respectively, and IIDG3 is connected to bus D, while IIDG4 is connected to bus E. All IIDGs have low-voltage ride-through capability. The load power factor is 0.9, using a constant power model. When the penetration rate of downstream IIDGs is 120% and 150%, simulation analyses are conducted on the measured positive-sequence components and protection actions as different faults occur along the line. Under normal operation, the maximum load current of the line is about 70 A, and the directional element will start when the measured current is greater than 140 A.

5.1. Penetration Rate of the Downstream IIDGs Is 120%

When the rated output power of both IIDG3 and IIDG4 is 727 kVA, the penetration rate of the downstream IIDGs is 120%. We set the following conditions to analyze. Case 1: Three-phase short circuit faults with transition resistance 0 Ω and 10 Ω occur in the middle section of line CD, f_1. Case 2: Three-phase short circuit faults with transition resistance 0 Ω and 10 Ω occur at 0.02 km away from bus C on line CD, f_2. Case 3: Phase-to-phase short circuit faults with 0 Ω and 10 Ω occur at f_1. Case 4: Phase-to-phase short circuit faults with 0 Ω and 10 Ω occur at f_2. The measured positive-sequence components and the actions of directional elements 1–8 under case 1 are shown in Table 3.

The data provided in Table 3 can be depicted on the coordinate circle shown in Figure 9. The measured voltages are located on the horizontal axis as the reference phasors, and different colored lines with arrows represent different current phasors while the length

denotes current amplitude. Circles with unequal intervals represent different current thresholds, and the angles represent the phase difference between the positive-sequence voltage and current. The green area is the action zone of the directional element, while the red area is the non-action zone. If the current phasor falls in the action zone, it means that fault occurs in the positive direction and the directional element acts. Conversely, if it falls in the non-action zone, the directional element will not act due to the reverse direction fault.

Table 3. The measured positive-sequence components and the actions of directional elements under case 1.

Fault Location	Transition Resistance	Measured Values and Actions of Directional Elements	1	2	3	4	5	6	7	8
f_1	0 Ω	Positive-sequence Voltage (V)	5177	3708	3708	2253	2253	323	323	363
		Positive-sequence Current (A)	1978	1979	1993	1994	2015	122	59	59
		Positive-sequence Impedance Angle (°)	70	−110	70	−110	69	44	−137	46
		Action of Directional Element	+	-	+	-	+	/	/	/
	10 Ω	Positive-sequence Voltage (V)	5737	5563	5563	5400	5400	5318	5318	5296
		Positive-sequence Current (A)	463	463	481	481	500	43	30	31
		Positive-sequence Impedance Angle (°)	12	−172	82	−175	5	−39	65	−114
		Action of Directional Element	+	-	+	-	+	/	/	/

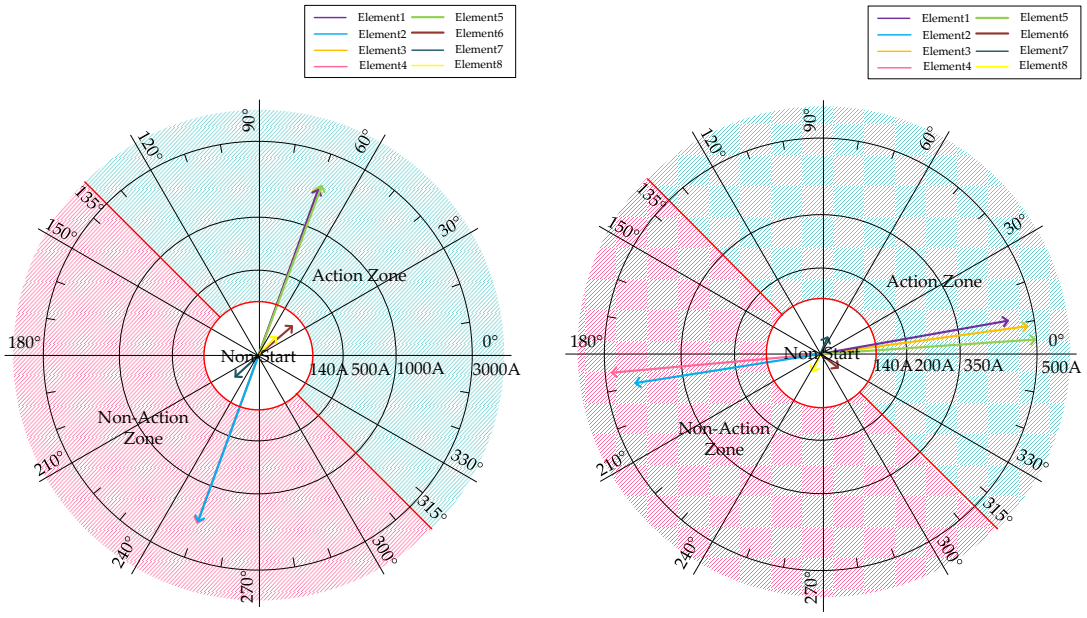

(**a**) (**b**)

Figure 9. (**a**) The measured electrical quantities and the actions of directional elements under case 1 when transition resistance is 0 Ω. (**b**) The results when transition resistance is 10 Ω.

The simulation results under cases 2–4 are shown in Figure 10, Figure 11 and Figure 12, respectively. Moreover, because fault occurs near bus C under case 2, the measured voltages by elements 4 and 5 are close to zero, and the prefault voltage phases are used to calculate the phase difference to avoid a voltage dead zone.

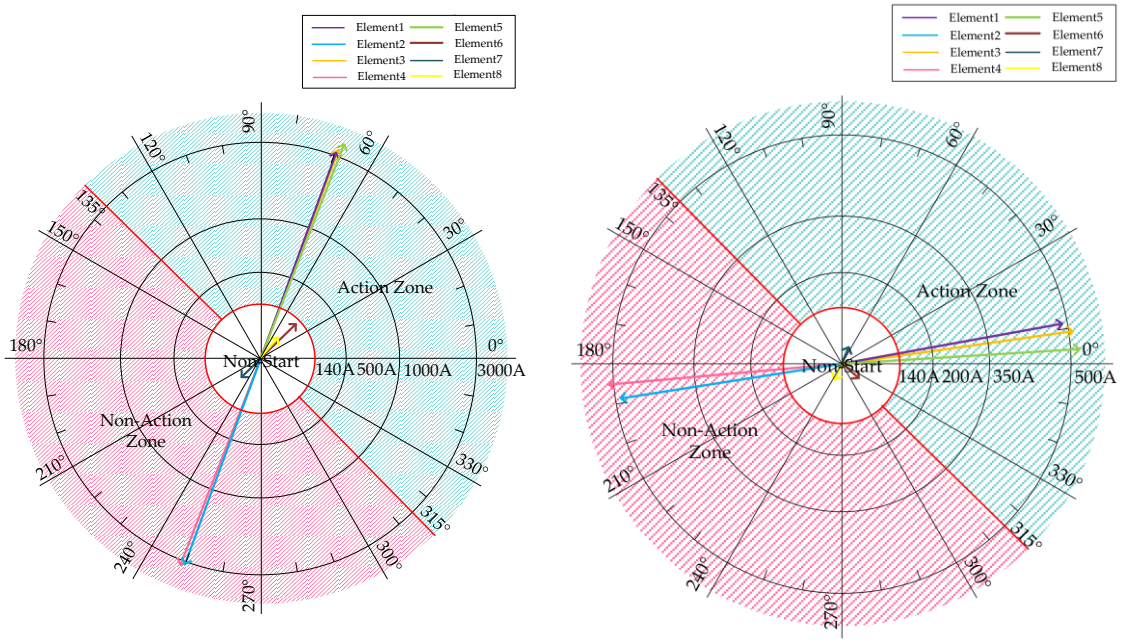

(**a**) (**b**)

Figure 10. (**a**) The measured electrical quantities and the actions of directional elements under case 2 when transition resistance is 0 Ω. (**b**) The results when transition resistance is 10 Ω.

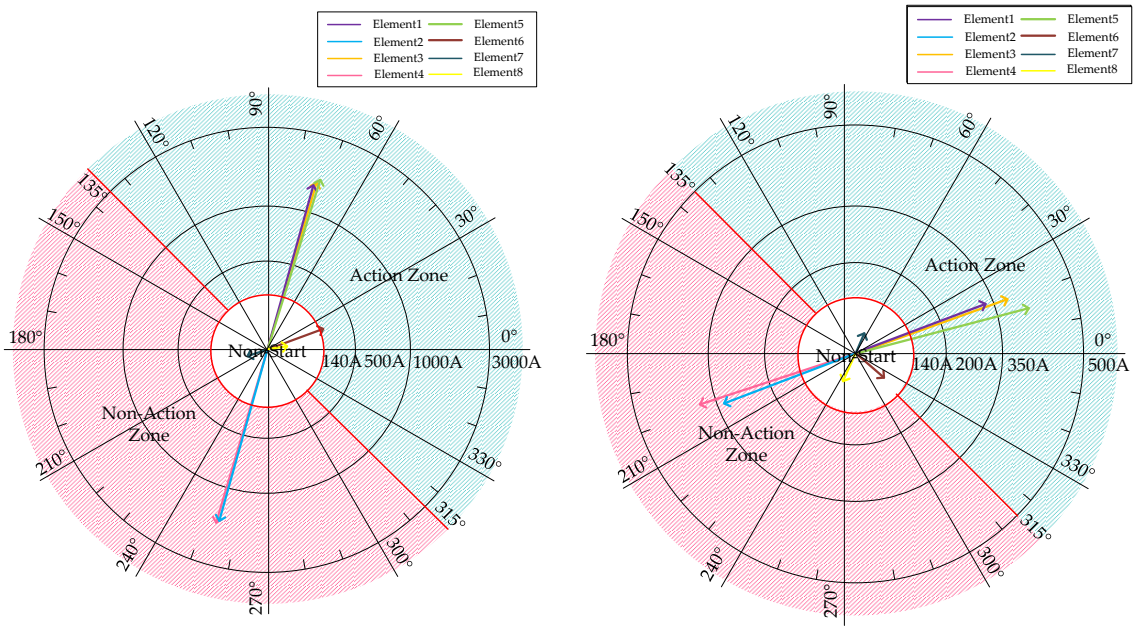

(**a**) (**b**)

Figure 11. (**a**) The measured electrical quantities and the actions of directional elements under case 3 when transition resistance is 0 Ω. (**b**) The results when transition resistance is 10 Ω.

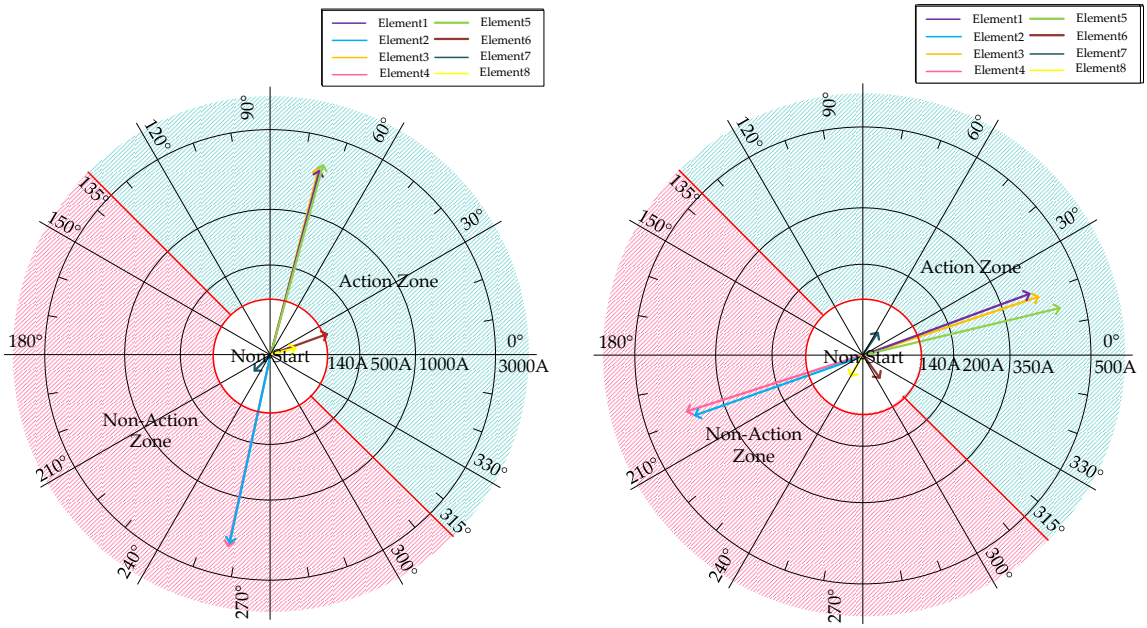

Figure 12. (**a**) The measured electrical quantities and the actions of directional elements under case 4 when transition resistance is 0 Ω. (**b**) The results when transition resistance is 10 Ω.

It can be seen from Figures 9–12 that the upstream directional elements can act correctly, while the downstream elements can correctly determine the fault direction in case the measured current causes a relay start; otherwise, they will be locked. The reason is that, for the downstream elements, the detected current value is always smaller than the specified starting value due to the lower penetration rate and limited output current of IIDG, preventing the element from starting no matter whether there is transition resistance or not. Specifically, in the case of transition resistance of 10 Ω, the measured positive-sequence impedance angle can be used to draw the conclusion that the downstream current flows to the load side, which is consistent with the analysis results in Section 4. If the starting conditions are not considered, the direction discrimination will be misjudged.

5.2. Penetration Rate of the Downstream IIDGs Is 150%

If the rated output power of both IIDG3 and IIDG4 is 909 kVA, the penetration rate of the downstream IIDGs is 150%. The simulations are carried out under the four cases in Section 5.1, and the results are shown in Figures 13–16.

Comparing the current values measured with different IIDG penetration rates under the same case, it can be found that the downstream current values increase with the penetration rate of IIDGs while the upstream current values slightly decrease, and it is consistent with the theoretical analysis. Comparing the measured positive-sequence impedance angles, it can be obtained that the upstream values have less change due to the constant direction of power flow. However, the downstream measurement value changes greatly because the downstream power flows to the fault location with the increase in IIDGs' capacity. Therefore, whether there is transition resistance or not, the action of the upstream directional elements will not be affected, while the downstream directional elements can act correctly as long as they can reach the starting condition.

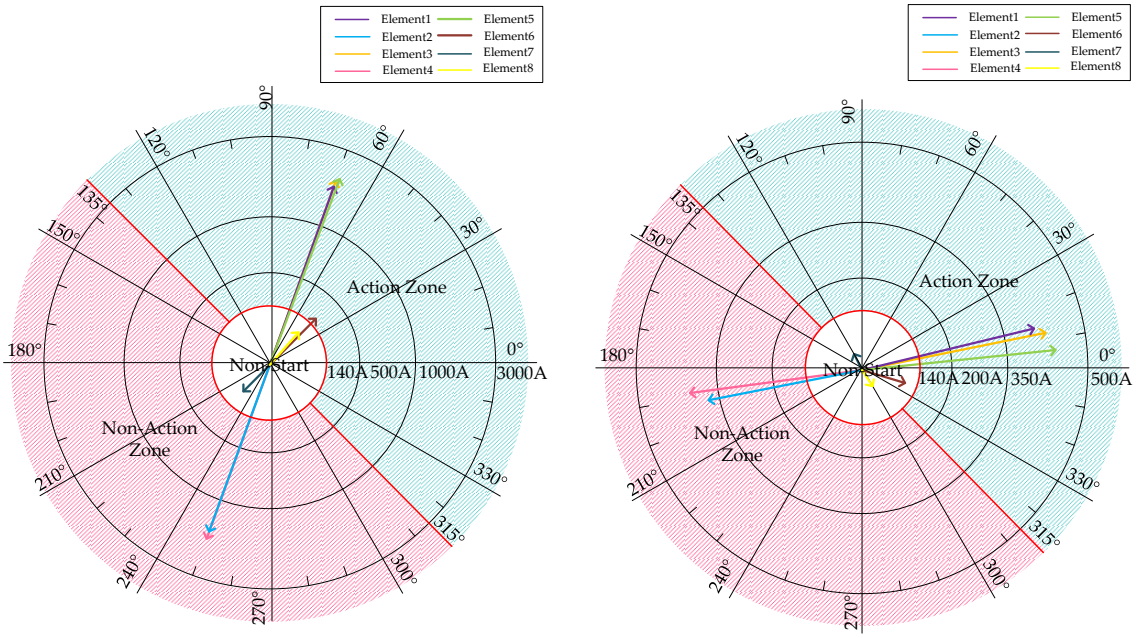

(**a**) (**b**)

Figure 13. (**a**) The measured electrical quantities and the actions of directional elements under case 1 when transition resistance is 0 Ω. (**b**) The results when transition resistance is 10 Ω.

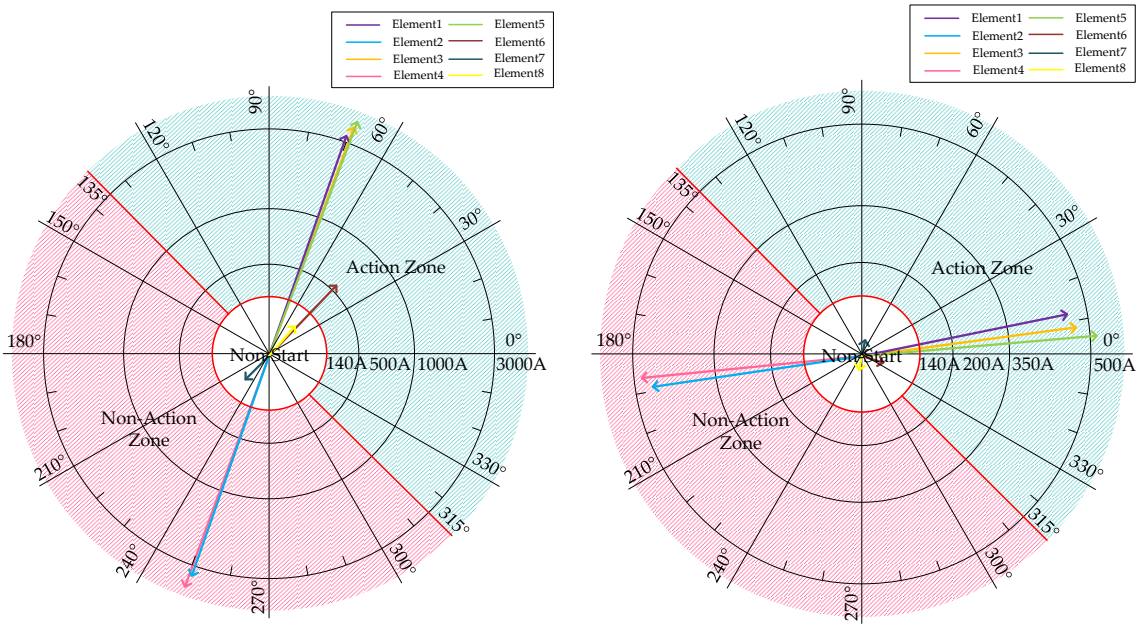

(**a**) (**b**)

Figure 14. (**a**) The measured electrical quantities and the actions of directional elements under case 2 when transition resistance is 0 Ω. (**b**) The results when transition resistance is 10 Ω.

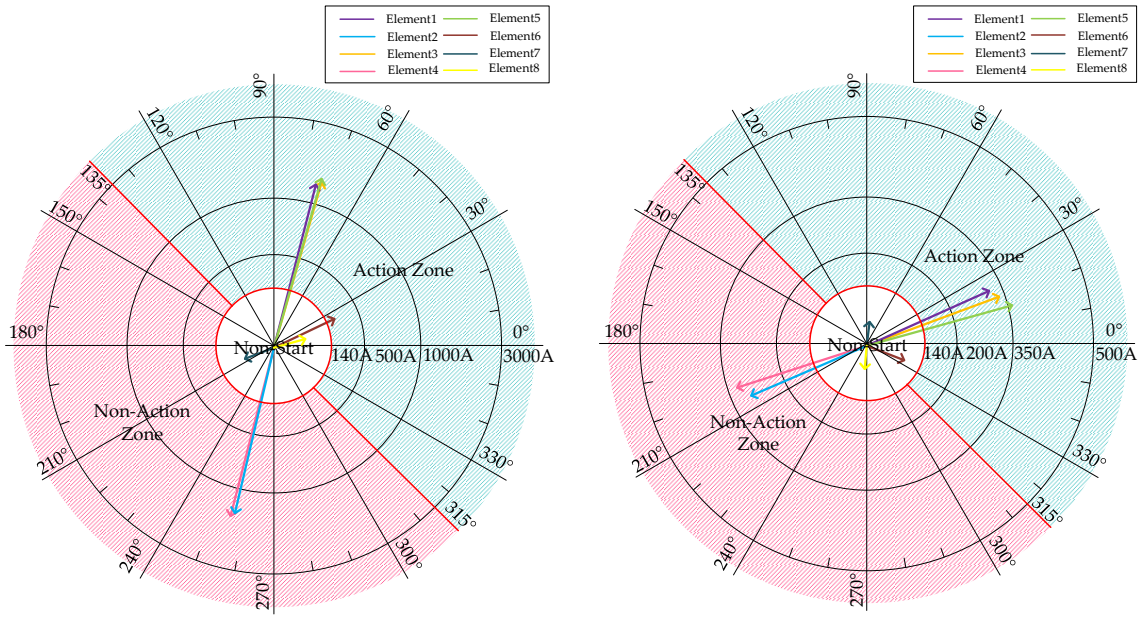

(**a**) (**b**)

Figure 15. (**a**) The measured electrical quantities and the actions of directional elements under case 3 when transition resistance is 0 Ω. (**b**) The results when transition resistance is 10 Ω.

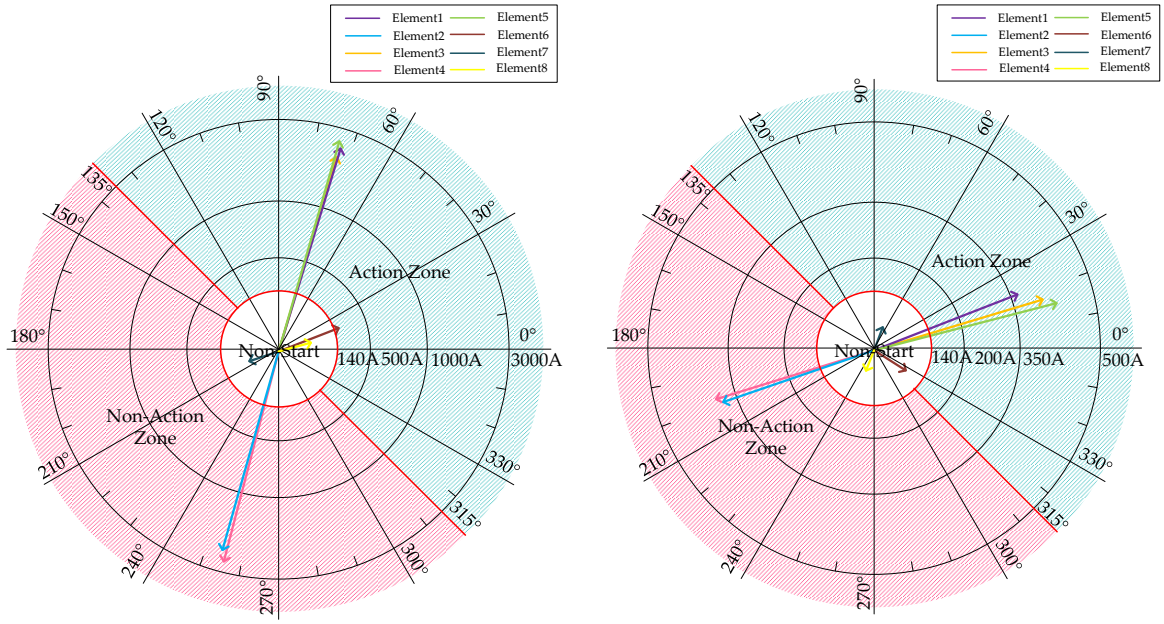

(**a**) (**b**)

Figure 16. (**a**) The measured electrical quantities and the actions of directional elements under case 4 when transition resistance is 0 Ω. (**b**) The results when transition resistance is 10 Ω.

6. Conclusions

To solve the problem of the poor reliability of the existing direction discriminations when IIDGs with low-voltage ride-through control are dispersively connected to a distribution network, a fault direction criterion based on post-fault positive-sequence components is proposed. The conclusions of this paper are as follows:

(1) The strong coupling nonlinear relationship between the output current of IIDG and the PCC voltage may lead to misjudgments of the directional elements based on 90° wiring and the positive-sequence fault components.
(2) The proposed direction criterion is a general criterion formed by extracting the post-fault positive-sequence components in the scenario of an IIDG multi-point grid-connected network considering a low-voltage ride-through strategy. It is suitable for fault direction discrimination when different short circuit faults occur at any position and is not affected by the prefault power flow. The direction criterion does not need to be adjusted when the system operation mode changes.
(3) The direction criterion can avoid misjudgment through the design of the start threshold when the system load is too large and the IIDG capacity is small, and can eliminate the dead zone using the prefault voltage phase, without affecting the direction discrimination result. It has a large margin, and can still operate correctly when the IIDG penetration is high and there is a short circuit through transition resistance.

Author Contributions: Conceptualization, F.Y. and G.H.; methodology, H.X. and S.F.; software, H.C.; validation, Y.L. and W.H.; writing—original draft preparation, S.F.; writing—review and editing, H.X.; project administration, F.Y. All authors have read and agreed to the published version of the manuscript.

Funding: This research was funded by the State Grid Hubei Electric Power Co., Ltd. (52153222001F).

Data Availability Statement: The data presented in this study are available on request from the corresponding author.

Conflicts of Interest: Authors Fan Yang, Hechong Chen, Gang Han, Yang Lei and Wei Hu were employed by the State Grid Hubei Electric Power Co., Ltd. The remaining authors declare that the research was conducted in the absence of any commercial or financial relationships that could be construed as a potential conflict of interest. The State Grid Hubei Electric Power Co., Ltd. had no role in the design of the study; in the collection, analyses, or interpretation of data; in the writing of the manuscript, or in the decision to publish the results.

References

1. Zhu, L.; Li, C.; Zhang, H.; Zhou, P.Y. Directional overcurrent protection for distribution systems containing distributed generation. *Power Syst. Technol.* **2009**, *33*, 94–98.
2. Wei, M.; Wang, C.; Yu, Y.; Liang, Y.; Wang, X. Optimal configuration scheme of multi-staged protection in distribution network for integration of high proportion of distributed photovoltaic. *Autom. Electr. Power Syst.* **2023**, *47*, 55–65.
3. Miao, X.; Zhao, D.; Liu, X.; Hong, C.; Zhuang, S. A Research review of short-circuit protection in distribution network with distributed generation. *High Volt. Eng.* **2023**, *49*, 3006–3019.
4. Wang, B.; Chen, H. Overview study on improving protection methods of distribution network with distributed generation. *Power Syst. Prot. Control.* **2017**, *45*, 146–154.
5. Yan, J.; Xia, S.; Wang, F. Analysis of new criterion for pilot direction of distribution network with distributed generations. *Proc. CSU-EPSA* **2018**, *30*, 112–117.
6. Zhou, C.; Zou, G.; Du, X.; Yang, J. A pilot protection method based on positive sequence fault component current for active distribution networks. *Proc. CSEE* **2020**, *40*, 2102–2112+2390.
7. Zhang, X.; Cao, R. *Solar Photovoltaic Grid-Connected Power Generation and its Inverter Control*, 3rd ed.; China Machine Press: Beijing, China, 2018; pp. 300–301.
8. Kong, X.; Zhang, Z.; Yin, X.; Wang, F.; He, M. Study on fault current characteristics and fault analysis method of power grid with inverter interfaced distributed generation. *Proc. CSEE* **2013**, *33*, 65–74+13.
9. Dai, Z.; Yu, L.; He, J.; Zhang, Y. Improvement strategy of local feeder automation for IIDG integration. *Electr. Power Autom. Equip.* **2023**, *43*, 184–191.
10. Li, Y.; Jia, K.; Bi, T.; Yan, R.; Chen, R.; Yang, Q. Influence mechanism of inverter interfaced renewable energy generators on fault component based directional relay. *Power Syst. Technol.* **2017**, *41*, 3230–3236.
11. Rao, C.; Shao, W.; Xia, J. Research on the directional component using the current phase characteristics in distribution system. *J. Xian'an Polytech. Univ.* **2017**, *31*, 781–787.
12. Liu, K.; Li, Y. Study on Solutions for Active Distribution Grid Protection. *Proc. CSEE* **2014**, *34*, 2584–2590.
13. Lin, X.; Lu, Y.; Wang, L. New current protection scheme considering distributed generation impact. *Autom. Electr. Power Syst.* **2008**, *32*, 50–56.

14. Si, X.; Chen, Q.; Gao, Z.; Ma, J.; Chen, M.; Wang, L. Protection scheme for active distribution system based on directions of current phase angle variation. *Autom. Electr. Power Syst.* **2014**, *38*, 97–103.
15. Li, Z.; Ye, S.; Wang, Q. Directional element of current for active distribution network. *High Volt. Appar.* **2018**, *54*, 199–204.
16. Zhu, Y.; Zhao, H.; Chen, Z. Fault direction discriminating element used for the distribution network with IIG integration. *Electr. Power* **2019**, *52*, 76–82.
17. Jalilian, A.; Hagh, M.T.; Hashemi, S.M. An innovative directional relaying scheme based onpostfault current. *IEEE Trans. Power Deliv.* **2014**, *29*, 2640–2647. [CrossRef]
18. Mishra, P.; Pradhan, A.K.; Bajpai, P. Time-domain directional relaying using only fault current for distribution system with PV plant. *IEEE Trans. Power Deliv.* **2022**, *37*, 2867–2874. [CrossRef]
19. Zhang, H.; Li, Y.; Chen, X.; Niu, W. New criteria of directional component in distribution network with photovoltaic generator of low voltage ride through capability. *Autom. Electr. Power Syst.* **2015**, *39*, 106–112.
20. Jiao, Y.; Liang, X.; Jiang, C. Directional element action area calculation considering LVRT of grid-connected PV plant. *Electr. Power Autom. Equip.* **2017**, *37*, 20–24.
21. Technical Rule for Connecting Photovoltaic Power Station to Power Grid: Q/GDW1617-2015. Available online: http://www.doc88.com/p-33773164675858.html (accessed on 18 June 2024).
22. He, J.; Li, T.; Dong, X.; Li, B.; He, J. *Primciples of Relay Protection of Electric Power System*; China Electric Power Press: Beijing, China, 2018; pp. 56–58.
23. Xu, B.; Li, T.; Xue, Y. *Relayig Protection and Automation of Distribution Networks*; China Electric Power Press: Beijing, China, 2017; pp. 114–116.
24. Chen, H.; Pan, X.; Huang, H.; Sun, X.; He, D.; Yong, C. Equivalent modeling of LVRT and current limiting links for distributed photovoltaic and wind turbine generators. *Electr. Power Autom. Equip.* **2022**, *42*, 25–32+39.
25. Math, B.; Fainan, H. *Integration of Distributed Generation in the Power System*; China Machine Press: Beijing, China, 2015; pp. 255–267.
26. Li, Z.; Xu, Y.; Wang, P.; Xiao, G. Restoration of a multi-energy distribution systems with joint district network recon figuration by a distributed stochastic programming approach. *IEEE Trans. Smart Grid* **2024**, *15*, 2667–2680. [CrossRef]